phys. stat. sol. (a) 72, 483 (1982)

Subject classification: 1.1 and 10.2; 22.1.1; 22.1.2

Institute of Solid State Physics, Academy of Sciences of the USSR, Chernogolovka[1] *(a) and I. V. Kurchatov Institute of Atomic Energy, Moscow*[2] *(b)*

Change of Interference Pattern in the X-Ray Section Topography of Single Crystals with Increasing Dimensions of an Incoherent Source

By

V. V. ARISTOV (a), V. G. KOHN (b), V. I. POLOVINKINA (a), and A. A. SNIGIREV (a)

The role of the non-monochromaticity of the radiation as well as of the source dimensions is analyzed in the X-ray section topography of single crystals. It is shown that for usual experimental conditions when the film is placed directly behind the crystal, the slit in front of the crystal really plays the part of an incoherent source, and the distance between the real source and the crystal has no affect on the interference pattern. A new type of interference pattern is revealed experimentally while changing the slit dimensions. The experimental results agree with theoretical computations.

Проведен анализ роли немонохроматичности излучения и размеров источника в рентгеновской секционной топографии монокристаллов. Показано, что для стандартных условий эксперимента, когда пленка помещена сразу за кристаллом, щель перед кристаллом играет роль некогерентного источника, а расстояние между реальным источником и кристаллом не влияет на вид интерференционной картины. Экспериментально обаружен новый тип интерференционной картины, возникающий при увеличении размеров щели. Экспериментальные результаты согласуются с теоретическими расчетами.

1. Introduction

In section topography of nearly perfect crystals a "point source" of spherical waves is simulated by a narrow slit placed in front of the crystal while the real X-ray source is at a distance of some tens of centimeters and its dimensions are 40 to 100 μm. On the other hand, the spectral width of a characteristic radiation line is, as known, sufficiently large in order for the radiation to be regarded as monochromatic provided the film is positioned immediately behind the crystal. Therefore, it is evident that in the section topographs the aspect and the contrast of the interference pattern have to be both greatly dependent upon such parameters of experimental scheme as the source-to-crystal distance, the crystal-to-film one, the width of the slit in front of the crystal, and the focal size of the X-ray tube as well as the spectral composition of the radiation.

Theoretical and experimental investigations of this dependence have been performed in a number of papers [1 to 7]. If the influence of the radiation non-monochromaticity on the aspect of the interference pattern is excluded either by the use of a special geometry of the experiment [2] or by pre-monochromatization [7] the aspect of diffraction pattern turned out to be strongly dependent on the relationship

[1] 142432 Chernogolovka, Moscow District, USSR.

[2] 123182 Moscow, USSR.

between the source-to-crystal-to-film distance (L) and the crystal thickness (t). For $t \gg t_s$ (where t_s is the characteristic thickness proportional to L) the interference pattern of a wedge-shaped crystal takes the form of alternating bright and dark fringes produced in the region of small thickness and which does not depend on L. The geometry of the interference fringes is described in this case by the Kato theory [8]. At $t \ll t_s$ the fringes are of the anomalous type [4, 5, 7]. Qualitatively such a pattern is described by the diffraction theory in the approximation of the incident plane wave. At $t \approx t_s$ we observed the effect of diffraction focusing of the slightly absorbing field [2] predicted theoretically in [1]. The role of the entrance slit placed in front of the crystal resulted in this case merely in the limitation of the frequency interval that forms the diffraction pattern, and diffraction by a slit can be neglected [6].

In a standard experimental setting of the section topography [9] when the incident radiation is non-monochromatic and the film is placed immediately behind the crystal the entrance slit in front of it changes the interference pattern. In the area of small crystal thicknesses at $t < 2a/\text{tg}\,\theta_B$, where $2a$ is the width of the entrance slit and θ_B the Bragg angle, a geometric image of the slit is observed [6], and provided $t > 2a/\text{tg}\,\theta_B$ the interference pattern is seen on the topographs [10] which is well described by the Kato theory [8], with no allowance made for the distance L.

The role of the entrance slit in the section topography of single crystals was studied, and results are presented in this paper. In Section 2 it is shown that in the case of a broad spectral line of radiation or an extensive source the slit in front of the crystal acts as an incoherent radiation source. Such a model enables us to give a simple interpretation of the effect of a geometric image of the slit and explains well the other details of experimental topographs.

The results of experimental studies as well as the topographs are exhibited in Section 3. The appearance of new details in the structure of interference fringes is seen with increase in the width of the slit that serves as an incoherent source in this case. Experimental topographs are compared with computed ones.

2. Slit as an Incoherent Source — Theory

If the distance between crystal and film is small, the experimental diffraction pattern is actually determined by the distribution of the reflected wave intensity at the exit surface of the crystal. In order to solve the problem of the X-ray spherical wave diffraction it is convenient to use in this case the formalism of the influence function [11 to 13].

The amplitude of the X-ray wave field in front of the crystal has the form

$$\boldsymbol{E}^{(\text{in})}(\boldsymbol{r}) = \exp\,[i\boldsymbol{K}_0\boldsymbol{r}]\,\boldsymbol{E}_0^{(\text{in})}(x, z)\,, \tag{1}$$

where $\boldsymbol{K}_0$ is the wave vector, the modulus of which is $K_0 = \omega_0/c$ and of which the direction satisfies the Bragg condition $K_h^2 = K_0^2$. Here $\boldsymbol{K}_h = \boldsymbol{K}_0 + \boldsymbol{h}$; c is the light velocity in the crystal, ω_0 the frequency corresponding to the maximum intensity in the spectrum, $\boldsymbol{h}$ a vector of the reciprocal lattice.

The field in the crystal is

$$\boldsymbol{E}(\boldsymbol{r}) = \exp\,[i\boldsymbol{K}_0\boldsymbol{r}]\,\boldsymbol{E}_0(x, z) + \exp\,[i\boldsymbol{K}_h\boldsymbol{r}]\,\boldsymbol{E}_h(x, z)\,. \tag{2}$$

Choosing the origin of coordinates at the entrance surface in the point of its intersection with the base path (see Fig. 1 of [6]) plotted from the source centre (see Fig. 1) and drawing the z-axis into the crystal normally to the surface for the symmetrical case, when vectors $\boldsymbol{K}_0$ and $\boldsymbol{K}_h$ form equal angles with the crystal surface, we arrive

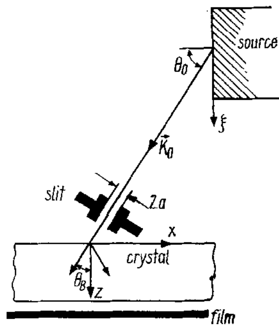

Fig. 1. Choice of a coordinate system in the crystal and on the surface of the X-ray source. Base path coincides with $\boldsymbol{K}_0$

at the following expression:

$$E_h(x, z) = \frac{B}{2i} \exp [iAz] \int_{-a_1}^{a_1} \mathrm{d}x_1 \, R(x - x_1) \, E_0^{(\mathrm{in})}(x_1, 0) \, . \tag{3}$$

Here

$$R(x) = \begin{cases} \mathrm{J}_0\left(B \sqrt{l^2 - x^2}\right); & |x| < l \\ 0; & |x| > l \, , \end{cases} \tag{4}$$

$$B = \frac{K_0 \sqrt{\chi_h \chi_{\bar{h}}} \, C_\mathrm{s}}{2 S_\mathrm{B}}, \qquad A = \frac{K_0 \chi_0}{2 C_\mathrm{B}}, \qquad l = z T_\mathrm{B} \, , \qquad a_1 = \frac{a}{C_\mathrm{B}} \, , \tag{5}$$

where $S_\mathrm{B} = \sin \theta_\mathrm{B}$, $C_\mathrm{B} = \cos \theta_\mathrm{B}$, $T_\mathrm{B} = \mathrm{tg}\, \theta_\mathrm{B}$, $\mathrm{J}_0(x)$ is the Bessel function of zeroth order, χ_0 and χ_h are the zero and h-th Fourier components of the crystal polarizability $\chi = \chi_\mathrm{r} + i\chi_\mathrm{i}$. The directions of the polarization vectors are chosen in the ordinary way and C_s is the polarization factor equal to unity for σ-polarization and to $\cos 2\theta_\mathrm{B}$ for π-polarization. It is assumed in (3) that a slit of width $2a$ is placed in front of the crystal at right angles to the incident X-ray beam, the slit centre being on the base path (see Fig. 1).

For a spherical wave of frequency ω radiated by the atom situated in the focus surface of the X-ray tube at a distance ξ from its centre the field amplitude $E_0^{(\mathrm{in})}(x_1, 0)$ can be written as

$$E_0^{(\mathrm{in})}(x_1, 0) \approx \frac{1}{L} \exp [i \, \Delta K(L - x_1 S_\mathrm{B} - \xi S_0)] \times$$

$$\times \exp \left\{ i \frac{K_0}{2L} [(x_1 C_\mathrm{B})^2 + (\xi C_0)^2 - 2 x_1 \xi C_\mathrm{B} C_0] \right\}, \tag{6}$$

where L is the source-to-crystal distance, $\Delta K = K - K_0$; $K = \omega/c$, $S_0 = \sin \theta_0$, $C_0 = \cos \theta_0$; θ_0 is the angle between $\boldsymbol{K}_0$ and the outer normal to the source surface. Substituting (6) into (3) we obtain

$$E_h(x, z) = \frac{B}{2iL} \exp \left[-\frac{\mu_0 z}{2 C_\mathrm{B}} + i\varphi \right] \int_{-a_1}^{a_1} \mathrm{d}x_1 \, R(x - x_1) \times$$

$$\times \exp [i\alpha x_1 + i\beta x_1^2] \, , \tag{7}$$

where

$$\left.\begin{aligned}\varphi &= \Delta KL + \frac{K_0\chi_{r0}z}{2C_B} - \Delta K\xi S_0 + \frac{K_0}{2L}(\xi C_0)^2\,,\\ \alpha &= \alpha_1 + \alpha_2 = \Delta KS_B + \frac{K_0C_BC_0}{L}\,\xi\,, \qquad \beta = \frac{K_0C_B^2}{2L}\,,\end{aligned}\right\} \tag{8}$$

and $\mu_0 = K\chi_{i0}$ is the coefficient of X-ray absorption.

It is easy to notice that if we substitute $x_1 + x_{\omega c}$ for x_1 in (7) and $x + x_{\omega c}$ for x, where $x_{\omega c} = \Delta KT_BL/K_0C_B$, the amplitude of a field with frequency ω in a point $x + x_{\omega c}$ has only an additional phase $\Delta\varphi = -\beta x_{\omega c}^2$ as compared to that of frequency ω_0 in a point x. In this case the dependence of the intensity $I_h = |E_h|^2$ on the frequency leads to a shift of the coordinate x by $x_{\omega c}$ [6].

The real diffraction pattern taking into account the non-monochromaticity of the radiation and the dimensions of the source is described as follows:

$$\bar{I}_h(x) = \int_{-\infty}^{\infty} \frac{d\alpha_1}{2\pi}\, F_\omega(\alpha_1) \int_{-\infty}^{\infty} \frac{d\alpha_2}{2\pi}\, F_s(\alpha_2)\, I_h(x, \alpha)\,, \tag{9}$$

where $F_\omega(\alpha)$ is the spectral function, $F_s(\alpha)$ is a function which describes the aperture ratio of a source in point $\xi = L\alpha/K_0C_0C_B$. Taking (7) into account we have

$$\bar{I}_h(x) = \left(\frac{B}{2L}\right)^2 \exp\left[-\frac{\mu_0 z}{C_B}\right] \int_{-a_1}^{a_1} dx_1 \int_{-a_1}^{a_1} dx_2\, R(x - x_1)\, R^*(x - x_2)\, \times$$
$$\times \exp\left[i\beta(x_1^2 - x_2^2)\right] \Phi_\omega(x_1 - x_2)\, \Phi_s(x_1 - x_2)\,, \tag{10}$$

where

$$\Phi_{\omega,s}(x) = \int_{-\infty}^{\infty} \frac{d\alpha}{2\pi}\, F_{\omega,s}(\alpha) \exp\left[-i\alpha x\right]. \tag{11}$$

Let us consider the limiting case where the spectral width of incident radiation is sufficiently broad or the source dimension is large, so that we can neglect the dependence on α in $F_{\omega,s}(\alpha)$ and put $\Phi_{\omega,s}(x) = \delta(x)\, F_{\omega,s}$. Omitting the normalization factor we obtain

$$\bar{I}_h(x) = \frac{B^2}{4L^2} \exp\left[-\frac{\mu_0 z}{C_B}\right] \int_{-a_1}^{a_1} dx_1\, |R(x - x_1)|^2\,. \tag{12}$$

The dependence of the phase on the distance L that leads to the focusing and anomalous pendellösung effect [5] is absent in the integral of (12).

The result obtained allows a descriptive physical interpretation. Each point on the illuminated part of the entrance surface is considered as an elementary source of spherical waves, and the resulting intensity is obtained by summation of the intensity of various points in the same manner as for ordinary incoherent sources. Thereby, the distance between the real source and the crystal is taken into account in (12) in trivial way as a factor L^{-2}.[3])

[3]) Attention should be drawn to the fact that the slit becomes a source of spherical waves of width comparable to the extinction length Λ_s, or more faithfully to Λ_s^* (see expression (17) and conditions (14) to (16)).

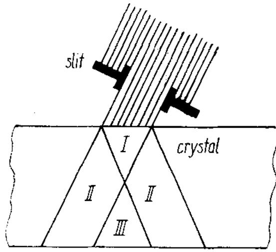

Fig. 2. The slit scheme image. I completely illuminated region, II image of the slit borders, III interference pattern on the slit

In the other limiting case at $F_\omega = \delta(\alpha - \alpha_1)$ and $F_s = \delta(\alpha)$ the slit becomes a coherent source at dimensions less than the first Fresnel zone $a_1 < \sqrt{\lambda L}$. In this case $\bar{I}_h(x) \approx \left| \int_{-a_1}^{a_1} dx_1\, R(x - x_1) \right|^2$. At $a_1 \gg \sqrt{\lambda L}$ the diffraction pattern is formed with the real source of radiation. In every intermediate case the intensity is described by (10).

The slit in front of the crystal naturally divides it into three regions which are shown in Fig. 2. In region I the integration limits in (12) are the same as in the absence of the slit. In this case we have for a non-absorbing crystal

$$\bar{I}_h = \frac{B^2}{4L^2} \int_{x-l}^{x+l} dx_1\, J_0^2[B\sqrt{l^2 - (x - x_1)^2}] = \frac{B}{4L^2} \int_0^{2Bl} dz\, J_0(z)\,. \tag{13}$$

This equation represents the common expression for the integrated intensity of reflected X-rays [14]. It follows from (13) that the main part of intensity is propagated along the directions of the incident and scattering waves [15], since the major contribution to the integral is made by the integration intervals where the argument of the Bessel function is small. In region II one of the integration limits is determined by the slit and this gives rise to a sharp decrease of the value of the integral by approximately a factor of two. Thus, (12) gives a natural interpretation of the effect of a geometric image of the slit [6]. In region III integration limits are determined entirely by the slit.

Let us consider conditions under which (12) is a good approximation. When characteristic radiation is used, the spectral function has Lorentz character, $F_\omega(\alpha) = 2\gamma_\omega/(\alpha^2 - \gamma_\omega^2)$, where $\gamma_\omega = \Gamma S_B/2c$, Γ is the halfwidth of the spectral line in terms of ω. In this case $\Phi_\omega(x) = \exp[-\gamma_\omega |x|]$. This function has a sharp peak of width $2/\gamma_\omega$. Thus, the first condition when (12) is reasonable, takes the form

$$a\gamma_\omega \gg C_B\,. \tag{14}$$

Practically, (14) is always fulfilled. Next, it is necessary that the function $R(x - x_1)$ would change slowly at the distance $2/\gamma_\omega$. Denote the range of essential change of this function by $\Delta_R(x, l)$. Then we have the condition

$$\gamma_\omega \Delta_R(x, l) \gg 2\,. \tag{15}$$

Finally, the third condition follows from the requirement that at distance $2/\gamma_\omega$ the exponential factor should change slowly. Based on (14) this condition can be written as

$$2a \ll A_\omega\,, \tag{16}$$

where $A_\omega = T_B L(\Gamma/\omega_0)$. In other words, the slit width must be less than the spectral width defined as the locus of points in the slit plane which correspond to the Bragg angles of incidence of rays for all frequencies in the spectral line. For example, for the

AuL_α line ($\lambda = 1.276$ Å) and Si(220) reflection we have $(\Gamma/\omega_0) = 4 \times 10^{-4}$ [16]; $\gamma_\omega^{-1} = \lambda/\pi S_B(\Gamma/\omega_0) = 0.3$ µm; $A_\omega = 140$ µm (at $L = 1$ m). In this manner, if the slit width is $2a = 10$ to 40 µm and $L > 50$ cm, both conditions (14) and (16) are met. As to the quantity $\Delta_R(x, l)$, its value essentially depends on the crystal thickness and the observation point. When $l \gg \Lambda_s^*$, where $\Lambda_s^* = \Lambda_s T_B$ and $\Lambda_s = \lambda C_B/|\chi_{rh}| C_s$ is the extinction length, $\Delta_R(x, l)$ is determined from the condition

$$\Lambda_s^* = |[l^2 - (x - x_1 - \Delta_R)^2]^{1/2} - [l^2 - (x - x_1)^2]^{1/2}| \,. \tag{17}$$

Assume, for example, that $x = x_1$. Then from (17) we have $\Delta_R \approx \Lambda_s^*(l/\Lambda_s^*)^{1/2}$. Therewith condition (15) is obviously fulfilled, since in the case considered $\Lambda_s^* = 6.8$ µm. If $x - x_1 = l$, then $\Delta_R \approx \Lambda_s^*(\Lambda_s^*/2l)$ and it follows from this that near the edges of the diffraction fringe condition (15) may break down as the crystal thickness increases. However, for a crystal thickness exceeding the extinction length not more than by a factor of six, (12) is a rather good approximation within the whole range of reflection. Note also that for thicker crystals the edges of the diffraction fringe are of no interest. Firstly, because the interference contrast vanishes there completely and, secondly, the intensity along the edges of a reflection fringe is determined by the normal absorption coefficient, and consequently it damps quicker than in the central part to which the Borrmann effect is applicable. Conventionally speaking, (12) can be used in this region, too.

An analogous situation arises also in the case when the source function $\Phi_s(x)$ has a sharp maximum. Let the source dimension be equal to A_s/C_0. Then $\Phi_s(x) = \sin(\gamma_s x)/\pi x$ with the maximum width $2/\gamma_s$, where $\gamma_s = A_s C_B/\pi\lambda L$. Conditions for γ_s and A_s are just of the same form (14) to (16) as for γ_ω and A_ω.

Notice that $A_s\gamma_s^{-1} = A_\omega\gamma_\omega^{-1}$. But in spite of the great similarity between the two cases there is one essential difference between them. In the case of an extended source A_s does not depend on L and $\gamma_s^{-1} \sim L$. Quite another situation occurs in the case of a broad spectral line of radiation when γ_ω^{-1} is not dependent on L and $A_\omega \sim L$. In this case for large source–crystal distances, $L \geqq 1$ m, the non-monochromaticity was found to be most significant, but for small distances L it is of the source dimensions. If $\gamma_\omega \approx \gamma_s$, the maximum width of the product $\Phi_s\Phi_\omega$ will be roughly half as less as γ_ω^{-1} which additionally increases the accuracy of the description according to (12).

3. A New Type of Interference Pattern

We have studied the diffraction pattern of symmetrical Laue reflections from dislocation-free, wedge-shaped Ge and Si crystals in the Lang scheme of the section topography [9]. The RU-3HM generator Rigaku Denki served as radiation source (focus size 40×200 µm²). We used the AuL_α characteristic radiation ($\lambda = 1.276$ Å). The specimens under study were positioned in the Lang camera of the A-3 Rigaku Denki type equipped with micrometer screws for the smooth opening of the slit in front of the crystal. The image was recorded on nuclear emulsion photographic plates such as MR and MK with a resolution of 200 and 375 lines/mm, respectively. The exposure time ranged from a few minutes to some hours depending on the slit width and the crystal thickness. In our scheme the distance from the X-ray source focus to the crystal is $L_1 = 108$ cm, the crystal–film distance $L_2 = 1$ to 2 cm.

Typical experimental images of a Si crystal in the case of the (220) reflection are shown in Fig. 3. With a slit width $2a \leqq 25$ µm we observed the conventional interference pattern of Kato and Lang [10], i.e. the system of alternating dark and bright contours of hyperbolic type with the vertex directed towards the wedge edge. The best resolution of the interference pattern was obtained for the smallest dimensions of the

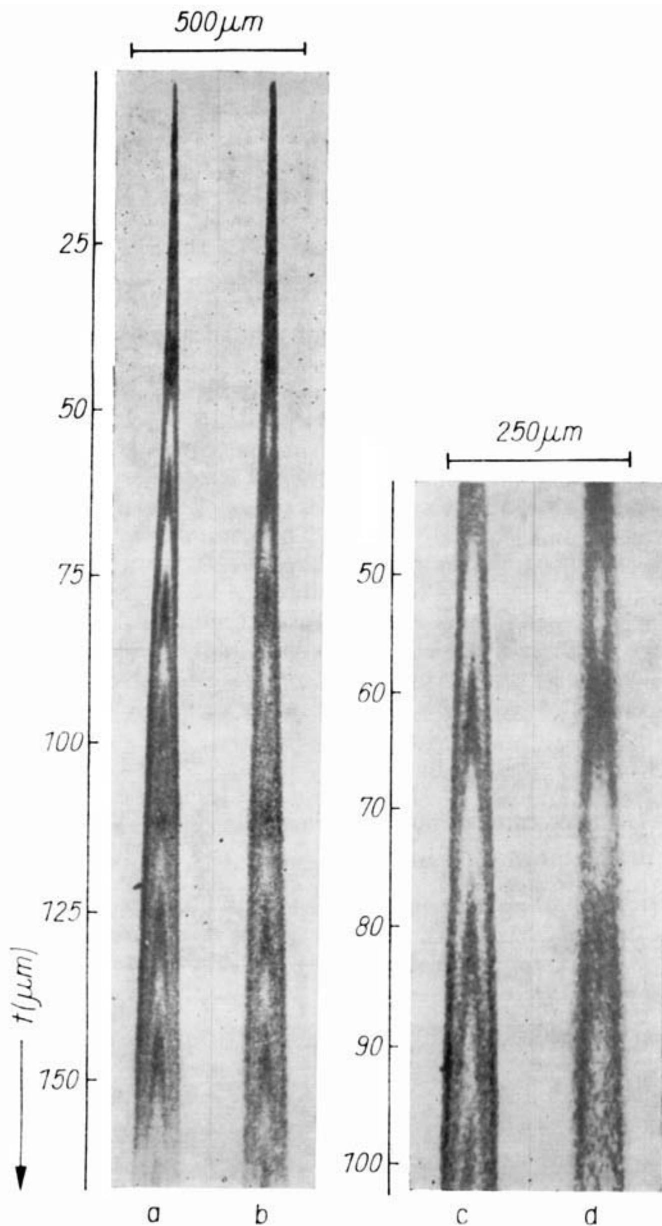

Fig. 3. Change in the interference pattern of a wedge-shaped Si crystal with increase in the slit dimension, (220) reflection, AuL_α radiation. a) and c) Experimental topograph and its enlarged fragment for the slit width $2a = 15$ µm; b) and d) the same for the slit width $2a = 25$ µm

slit, $2a = 5$ to 10 µm. Fig. 3a shows the topograph for the case of the slit size 15 µm. The crystal thickness corresponding to the focusing of the slightly absorbing mode of the wave field [1, 2] is in this case (for $L = 110$ cm) $t_g = 37$ µm. It is seen that the form of the interference pattern corresponds to the one which would appear at $L = 0$.

Thus, despite the fact that the diffraction by a slit can be ignored in this scheme, the aspect of the interference fringes in the topograph is not dependent on the distance L.

With increasing slit dimension up to $2a \geqq 40$ μm, the contrast of the interference pattern changed and passed into thickness fringes.

In the cases of intermediate slit width, $2a \approx 20$ to 30 μm, the reversal of the curvature of several (two or three) pendellösung contours was observed in the topograph area corresponding to the wedge thickness $t = 40$ to 90 μm like the case of the anomalous pendellösung effect (Fig. 3b).

Similar changes of the interference pattern were also observed for the Si(111) reflection: at $2a \leqq 15$ μm the Kato-Lang pattern was seen, at $2a \geqq 25$ μm — the thickness fringes, at $2a \approx 20$ μm — the reversal of the hyperbolae curvature.

For the Ge(220) reflection the reversal of the curvature of pendellösung fringes was observed at $2a \approx 15$ μm.

The change in the structure of interference fringes looks as if with increase in the slit dimensions in the middle of the picture of the normal pendellösung effect there appeared anomalous fringes which depend, as is known, on the source–crystal distance. However, the reversal of the curvature of pendellösung fringes was observed in the thickness range $t > t_s$ and besides, according to estimations given above, the slit in this case actually plays the role of an incoherent source. Thus, the observed change in the structure of the interference fringes is connected in reality with an increase in the dimensions of this source.

To be sure that such a situation is possible we have performed numerical computations of the interference pattern for Si(220) reflection with AuL_α radiation by formula (12) in the approximation of a non-absorbing crystal.

For computations it is convenient to write this formula in the form

$$\overline{I}_h(x, z) \approx \int_{A(x)}^{B(x)} dx_1 \sum C_s^2 J_0^2 (B \sqrt{l^2 - x_1^2}) , \tag{18}$$

where the integration is over the two states of polarization,

$$A(x) = \max(-l, x - a_1) , \qquad B(x) = \min(l, x + a_1) .$$

Results of computations for the thickness range 60 to 130 μm are shown in the form of a topographic map in Fig. 4. As is seen, with increase in the slit dimensions, i.e. with variation of the integration limits in (18), concurrently with the decrease in con-

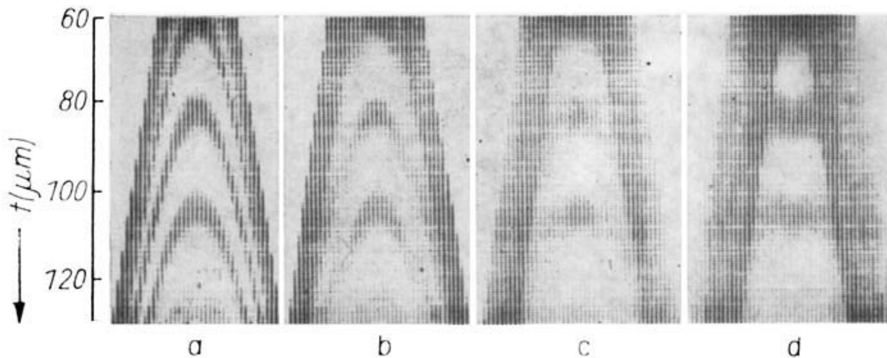

Fig. 4. Computed topographs of a wedge-shaped Si crystal, (220) reflection, AuL_α radiation. a) $2a = 2$, b) 10, c) 20, d) 30 μm. Computations were made with formula (18) for the thickness range 60 μm $\leqq t \leqq$ 130 μm

trast a change in the form of the pendellösung fringes themselves takes place, this change being in qualitative agreement with the results of the experiment. A further increase in the slit width brings about the formation of the thickness fringes.

Thus, the experiment verifies the conclusion that under conditions (14) to (16) the slit should be considered as an incoherent source of spherical waves. The analysis shows that the proposed theoretical model remains valid also for a more complicated case when the X-ray scattering occurs in two nearby crystals or in interferometers of various constructions.

4. Conclusion

The results presented in this paper clarify the question on the suitability of the Kato theory [8] for explaining experimental section topographs. This theory describes well the geometry of the interference pattern of section topographs though the theoretical assumption that the monochromatic point source is positioned on the crystal surface is obviously not met in the experiment. Radiation non-monochromaticity and greater source dimensions as compared to the slit width are the reasons why this theory is applicable for usual experimental schemes. The resulting diffraction pattern no longer depends on the distance between source and crystal and the slit plays the role of an incoherent source. In this case the influence of slit dimensions on the aspect of the diffraction pattern proved to be non-trivial. As the slit width increases, along with the decrease in the contrast the change in sign of the curvature of the interference fringes takes place, and next the thickness fringes are formed. The results obtained should be taken into consideration in analyzing the section topographs of crystals with defects.

Acknowledgement

The authors are thankful to Dr. E. V. Suvorov for help in the experiment.

References

[1] A. M. Afanasev and V. G. Kohn, Fiz. tverd. Tela **19**, 1775 (1977).
[2] V. V. Aristov, V. I. Polovinkina, I. M. Shmytko, and E. V. Shulakov, Zh. eksper. teor. Fiz., Pisma **28**, 6 (1978).
[3] V. D. Kozmik and I. P. Mikhailyuk, Ukr. fiz. Zh. **23**, 1570 (1978).
[4] V. V. Aristov and V. I. Polovinkina, Acta cryst. **A34**, 227 (1978).
[5] V. V. Aristov, V. I. Polovinkina, A. M. Afanasev, and V. G. Kohn, Acta cryst. **A36**, 1002 (1980).
[6] V. V. Aristov, V. G. Kohn, and V. I. Polovinkina, phys. stat. sol. (a) **62**, 431 (1980).
[7] V. V. Aristov, T. Ichikawa, S. Kikuta, and V. I. Polovinkina, Japan. J. appl. Phys. **20**, 1947 (1981).
[8] N. Kato, Acta cryst. **A14**, 526, 627 (1961); J. appl. Phys. **39**, 2225, 2231 (1968).
[9] A. R. Lang, J. appl. Phys. **29**, 597 (1958).
[10] N. Kato and A. R. Lang, Acta cryst. **12**, 787 (1959).
[11] I. Sh. Slobodetskii, F. N. Chukhovskii, and V. L. Indenbom, Zh. eksper. teor. Fiz., Pisma **8**, 90 (1968).
[12] A. Authier and D. Simon, Acta cryst. **A24**, 517 (1968).
[13] A. M. Afanasev and V. G. Kohn, Acta cryst. **A27**, 421 (1971).
[14] W. H. Zachariazen, Theory of X-Ray Diffraction in Crystals, Wiley, New York 1945.
[15] P. A. Besirganyan, Preprint, Some Questions of Optical Principles of the X-Ray Diffraction, Erevan Univ., Erevan 1976 (in Russian).
[16] I. H. Williams, Phys. Rev. **45**, 71 (1934).

(Received March 24, 1982)